Nanoscale

REVIEW

Biomedical nanomaterials for imaging-guided cancer therapy

Yuran Huang,[ab] Sha He,[a] Weipeng Cao,[b] Kaiyong Cai*[a] and Xing-Jie Liang*[b]

To date, even though various kinds of nanomaterials have been evaluated over the years in order to develop effective cancer therapy, there is still significant challenges in the improvement of the capabilities of nano-carriers. Developing a new theranostic nanomedicine platform for imaging-guided, visualized cancer therapy is currently a promising way to enhance therapeutic efficiency and reduce side effects. Firstly, conventional imaging technologies are reviewed with their advantages and disadvantages, respectively. Then, advanced biomedical materials for multimodal imaging are illustrated in detail, including representative examples for various dual-modalities and triple-modalities. Besides conventional cancer treatment (chemotherapy, radiotherapy), current biomaterials are also summarized for novel cancer therapy based on hyperthermia, photothermal, photodynamic effects, and clinical imaging-guided surgery. In conclusion, biomedical materials for imaging-guided therapy are becoming one of the mainstream treatments for cancer in the future. It is hoped that this review might provide new impetus to understand nanotechnology and nanomaterials employed for imaging-guided cancer therapy.

1. Introduction

Based on the persistent problem of cancer, various small scale tools developed in novel nanomedicine, including liposomes,

[a]College of Bioengineering, Chongqing University, 174 Shazheng Road, Shapingba, Chongqing, China. E-mail: kaiyong_cai@cqu.edu.cn; Fax: +86 23 6511 2619; Tel: +86 23 6511 2877

[b]Chinese Academy of Sciences Key Laboratory for Biological Effects of Nanomaterials and Nanosafety, National Center for Nanoscience and Technology of China, 11 Beiyitiao, Zhongguancun, Beijing, 100190, China. E-mail: liangxj@nanoctr.cn; Fax: +86-10-62656765; Tel: +86-10-82545569

polymers, micelles, metallic nanoparticles *etc.*, have drawn considerable research interest for their potential in bringing antitumor biomedicine into a new era.[1] Enormous amounts of evidence have shown that these nano-carrier materials are capable of improving the efficiency of therapeutic intervention. However, only relying on the self-functioning of nano-systems (EPR effects, pH sensitivity, enzymatic responsiveness, redox-sensitivity, recognition moieties) is not sufficient to match the changeable and complicated tumor microenvironment.[2] For instance, the interstitial pH of solid tumors is lower than that of normal tissues, which is the basis of many pH-sensitive

Yuran Huang

Yuran Huang received her BS of bioengineering at Chongqing University, China in 2010. She is pursuing her master's degree under the joint guidance of Prof. Kaiyong Cai (Chongqing University) and Prof. Xingjie Liang (National Center for Nanoscience and Technology (NCNST)). Her research interest is nanomaterials-based (especially gold and magnetic nanoparticles) multimodal imaging and cancer therapy (theranostics), and she also focuses on silica/polymer-based controllable drug delivery systems.

Sha He

Sha He was born in 1988 in Hunan, China and received his BS at Huazhong University of Science & Technology in 2009 and his MS at Chongqing University in 2012, both in biomedical engineering. He conducted his master's study and research under the joint guidance of Prof. Kaiyong Cai (Chongqing University) and Prof. Xingyu Jiang (NCNST). His research interest is focused on nanoparticle-based in vitro *and* in vivo *diagnostics.*

nanocarriers developed to deliver drugs to tumors.[3] However, the microenvironment only becomes sufficiently acidic 100 μm beyond a blood vessel wall for those particles that take advantage of pH-responsiveness.[4]

Considering those disadvantages, imaging, as a visualization technique, was introduced to the development of nanocarriers. Those materials can act as both therapeutic agents and imaging contrast agents. As previous studies have demonstrated, imaging paved the way to visualize the behaviour of nanoparticles in metabolic pathways and control the response to external stimuli, such as magnetic field, heat, light and ultrasound. This progress in biomedicine would realise early personalized diagnosis and subsequent specific therapy to maximize the efficiency of therapeutic agents. In this review, we will summarize different kinds of nanomaterials used in current single mode imaging methods and multi-modality imaging. Furthermore, the potential application of biomedical nanomaterials for imaging-guided cancer therapy will be introduced in detail.

2. Conventional single-modal imaging

To date, five types of imaging modalities can be employed to visualize targeted cells and/or molecules, including nuclear imaging (positron emission tomography (PET) and single photon emission computed tomography (SPECT)), X-ray computed tomography (CT), magnetic resonance imaging (MRI), optical imaging, and ultrasound imaging (US imaging).[5] These imaging modalities can be broadly divided into two categories: CT, MRI and US, characterized by high spatial resolution, are classified as primarily morphological/anatomical imaging techniques, while others capable of detecting molecular and cellular changes of diseases are categorized into primarily molecular imaging techniques.[6] In real clinical detection and treatment, all those five imaging modalities make a significant contribution as irreplaceable accessories for doctors. However, those techniques have different advantages and disadvantages (Fig. 1) considering various parameters, such as spatial/depth resolution and sensitivity.

2.1. Nuclear imaging

Nuclear imaging is a method based on nuclear magnetic resonance (NMR) technology. Both PET and SPECT are quantitative nuclear imaging methods providing images of the *in vivo* distribution of injected radioisotopes. They favour information on biological function to anatomical structure. Nevertheless, there are some differences between PET and SPECT imaging. Firstly, SPECT allows the labelling of different radioisotopes for two or more compounds simultaneously, and the common radioisotopes it uses are able to influence the structure and function of biomolecules. Secondly, PET particularly possesses higher sensitivity than SPECT, capable of evaluating low levels of cellular activity.[7] In addition, the detectable area in small

Dr Weipeng Cao received her B.M. at the Department of Medicine, Shandong University. She finished her PhD at School of Life Sciences, Tsinghua University and worked as an assistant researcher at the CAS Key Laboratory for Biomedical Effects of Nanomaterials and Nanosafety, NCNST. Her research interests: using molecular biology, cell biology and biochemistry methods, combined with nanotechnology, to study the biological effects of nanomaterials and their functions in animals, cellular or molecular levels.

Weipeng Cao

Dr Kaiyong Cai, Professor of Biomedical Engineering, received his PhD degree in Tianjin University in 2002. Then, he spent 3 years in the Institute of Materials Science & Technology, Friedrich-Schiller-Jena University for postdoctoral research. He joined Chongqing University in 2005. His main research interest focuses on titanium, functionalized bio-interfaces and drug delivery systems. He has published more than 60 research papers in peer reviewed international journals.

Kaiyong Cai

Dr Xing-Jie Liang received his PhD at the National Key Laboratory of Bio-macromolecules, Institute of Biophysics at CAS. He finished his postdoctoral studies at the Center for Cancer Research, NCI, NIH, and worked as a Research Fellow at the Surgical Neurology Branch, NINDS. He worked on Molecular imaging at the School of Medicine, Howard University before he became deputy director of CAS Key Laboratory for Biomedical Effects of Nanomaterials and Nanosafety, NCNST. Developing drug delivery strategies for prevention/treatment of AIDS and cancers are current programs ongoing in Dr Liang's lab based on understanding of basic physico-chemical and biological processes of nanomedicine.
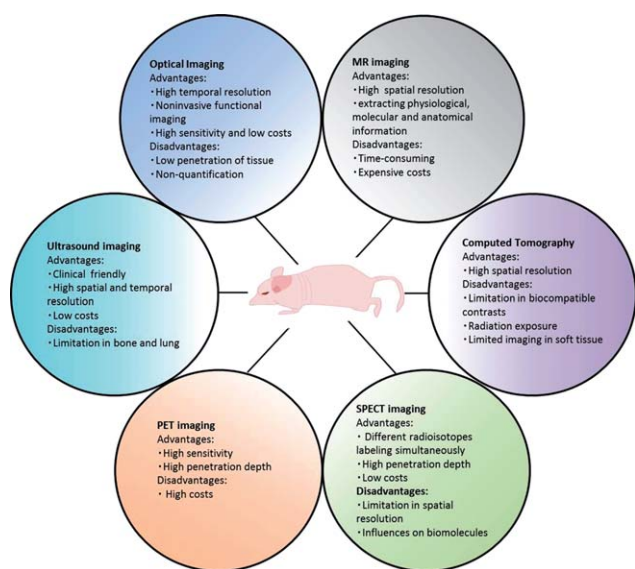
Xing-Jie Liang

Fig. 1 Advantages and disadvantages of different molecular imaging techniques.

animals and the spatial resolution are different between PET and SPECT. PET measures ~ 4 to 8 mm^3 and SPECT ~ 12 to 15 mm^3 in small animal imaging systems, PET has a spatial resolution of ~ 1 to 2 mm^3 and SPECT $\sim 1 \text{ mm}^3$.[8] Finally, SPECT is much lower-cost than PET in clinical applications.

^{11}C, ^{13}N, ^{15}O, ^{64}Cu, ^{124}I and ^{18}F are common radioactive contrast agents for PET, while ^{99m}Tc, ^{111}In for SPECT. These isotopes all require chelating moieties in the labelling of compounds, such as ^{11}C-raclopride, ^{18}F-FDDNP, ^{18}F-FDG (fluorodeoxyglucose), ^{64}Cu-DOPA and ^{111}In-monoclonal endoglin, ^{99m}Tc-sestamibi, ^{131}I-Altropane.[9,10] Nowadays, researchers basically use nanocarriers to manipulate the behavior of nuclear isotopes in the biological environment.

2.2. Computed tomography

CT is a sensitive imaging method for detection the density of absorption of X-rays in different tissues when crossing through the body of the subject.[11] It is a completely non-invasive procedure with high-contrast resolution, which can even distinguish tiny differences in physical density of less than 1% between tissues. However, CT has very limited choices for compatible contrast agents so that it essentially cannot be used to label molecules, and it has a low detection sensitivity.[12] Additionally, radiation exposure during CT examination is the biggest disadvantage, because it probably bring some unpredictable harm to patients, especially to children.[13] However, the benefits of CT still outweigh the risk in many cases, which endows its irreplaceable status in clinical diagnosis.

Various contrast media have been developed over the years and used along with CT imaging. Barium sulfate suspension and water-soluble aromatic iodinated contrast agents, currently most common ones approved for human use, have a very low retention rate and are not tissue-specific. Thus, some recent nanotechnology-based contrast agents have emerged and showed their promising future. Popovtzer's group synthesized gold nanorod-

based CT contrasts, which conjugated with UM-A9 antibodies to specifically target head and neck cancer.[14] Kim *et al.* also utilized gold nanoparticles as contrast agents for CT imaging. They prepared long circulating PEG-coated gold nanoparticles in bloodstream, and their results indicated that PEG-gold nanoparticles had approximately two-fold high contrast in tumor than normal tissue on CT images.[15] Moreover, fullerenes and carbon nanotubes also can be applied in X-ray CT.[16] With recent advancements in nanoparticle-based contrast media, the role of CT imaging in biological research is being refined.

2.3. Magnetic resonance imaging

MRI is a non-invasive imaging technique also based on the property of NMR to visualize with excellent anatomical detail and soft tissue contrast.[17] During the MRI procedure, the active nuclei excited by a selective radio-frequency (RF) pulse will "relax" immediately back to their initial state. This relaxation process can be divided into two components, longitudinal relaxation time (T_1) and transverse relaxation time (T_2), each of which can be used to generate an MR image with discrimination between different types of tissue. Some primary parameters varied in different tissues corresponding to the amount of signal and the extent of contrast, as shown in Table 1. MRI measurement is time-consuming and expensive, but is still superior for its high spatial resolution in three-dimensions, high contrast between soft tissues and simultaneous extraction of physiological, molecular and anatomical information.[18] This is why it is studied and promoted by many researchers.

Essential MRI contrast agents visualise the analysis of biological information and the diagnosis of diseases in an economical and practical way. Most of the presently available MRI contrast agents are paramagnetic complexes, usually gadolinium (Gd^{3+}) chelates. Gd-DTPA has been the most widely used.[19] However, for clinical use, repeated injections with high dosage are often required for these chelates to elongate their blood circulation time, which will bring in inaccuracies from false-positive contrast enhancement. Over the last decades, many scientists have focused on developing novel MRI contrast agents, including nanoparticles with uniform size (Fig. 2), with enhanced relaxation properties and biocompatibility.[20,21] Superparamagnetic iron oxide (SPIO) received great attention as a nanoparticle contrast agent, and some products have been approved by the FDA or are in clinical trials.[22] SPIO is mostly used in T_2 contrast agents, however, extremely small-sized iron oxide nanoparticles (ESIONs) with sizes less than 4 nm were also proved as the candidates for T_1-weighted imaging without the "blooming effect" of T_2-weighted imaging and toxicity of normal nanoparticle T_1 contrast agents.[23] Besides iron oxides, alloyed nanoparticles are another candidate with more efficient T_2 contrast effects. Various bimetallic ferrite nanoparticles, such as $CoFe_2O_4$,[24] $MnFeO_4$,[25] $NiFe_2O_4$,[26] have been tested as T_2 contrast media. Their relaxivities are several times higher than those of pure Fe_3O_4 nanoparticles. Moreover, on the basis of Gd-contrast agents, nanoparticle Gd-based contrast media also have been investigated, including Gd_2O_3,[27] GdF_3[28] and $GdPO_4$,[29] mostly enhancing the signal of T_1-weighted MR imaging. Recently, MnO[30] and hollow structured manganese oxide nanoparticles were reported as new MRI contrast agents. Hyeon

Table 1 The parameters which influence the signal of MRI[a]

Factors	Description	Contrasts	Applied to	Images
T_1	Spin–lattice/longitudinal relaxation	Paramagnetic contrasts (Gd^{3+} chelates, MnO, Gd-based NPs)	The regions containing rapidly tumbling free water molecules (e.g. brain, blood)	Enhance MRI signal
T_2	Spin–spin/transverse relaxation	Superparamagnetic contrasts (SPIO, Fe-based alloy NPs)	The molecules containing high concentration of hydrogen nuclei	Reduce MRI signal
T_2^*	Total relaxation	Ferromagnetic iron oxide NPs	Same as T_2-weighted MR imaging	Reduce MRI signal

[a] T_2 is affected by T_2^* and relaxation of inhomogenous magnetic field produced from tissue-inherent factors or an external source: $\frac{1}{T_2^*} = \frac{1}{T_2} + \gamma B_s$; γB_s is susceptibility effects representing the relaxation by the field inhomogeneities.
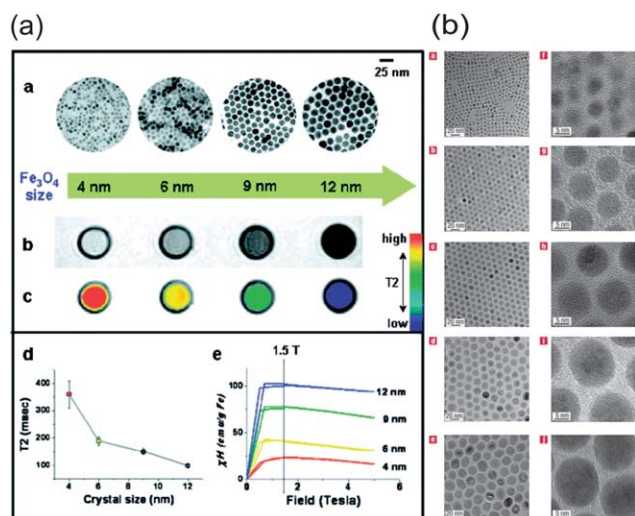

Fig. 2 (a) Size effects of water-soluble Fe_3O_4 nanocrystals on magnetism and MR signals; (b) TEM images of different oleic-Fe_3O_4 nanoparticles.[20,21]

et al. synthesized various hollow oxide nanoparticles via nano-scale acid etching using MnO as the starting material and alkylphosphonic acid impurity as the etchant. These nanoparticles show spin relaxation enhancement effect while dispersed in water.[31]

Most newly developed nanoparticles for MRI are still in the stage of in vivo or preliminary animal studies. Many issues should be clearly addressed before clinical application, including biocompatibility, long circulation and pharmacokinetics. However, these researches are still helpful for personalized therapy in the future.

2.4. Optical imaging

Optical imaging is an imaging technique based on the behavior of visible, ultraviolet and infrared light. This imaging technique could be divided into bioluminescence imaging and fluorescent imaging and both of them have the advantages of high temporal resolution, noninvasive functional imaging, high sensitivity and low cost. Bioluminescence imaging (BLI), utilizing native light emission generated by chemiluminescent reaction between an enzyme and its substrate, is allowed simultaneously quick and easy localization and serial quantification of ongoing biological/molecular processes in living experimental models.[32] This technology has been applied in studies to monitor transgene expression, transplantation, toxicology, viral infections, and gene therapy.[33] Unlike BLI, fluorescence imaging is based on the absorption of energy from external light of one wavelength by a fluorophore such as a fluorescent proteins. On account of the stability and distinction of the fluorescent proteins by color, fluorescence imaging is increasingly attractive in disease detection.[34–36] However, it is still limited by its properties of non-quantification, surface information and especially low penetration caused by the main absorption in the visible light range. These are the primary reasons that have boosted the rapid advances in near-infrared fluorescent probes.

Near-infrared (NIR) light (650–950 nm) is minimally absorbed in biological tissues and physiological fluids (for example, skin and blood), so that it helps to maximize the efficient penetration depth compared to visible light in living tissues. With different microwatt NIR lasers, it can penetrate almost 7 cm through muscle tissues, and 10 cm through breast tissue (Fig. 3).[37,38] Therefore, many different imaging probes tuned in the NIR window have been developed for visualization, and displayed promising applications in cancer treatment.[39,40] Moreover, combining NIR optical imaging with nanotechnology is also another non-negligible way to improve the detection limits and clinical effectiveness of optical imaging. Those progresses in nanotechnology have paved the way for early diagnosis, therapy and prevention of diseases, particularly tumors.

Over the past several years, many different kinds of nano-structures, including quantum dots (QDs), gold-based nano-structures etc., are synthetically tuned to extinguish light in the
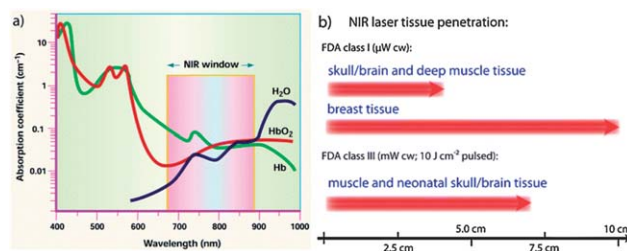

Fig. 3 (a) The wavelength range of NIR window; (b) the maximum penetration depths in tissues of external NIR laser radiation.[37,38]

NIR light window. For QDs, those semiconductor nanoparticles possess novel electronic, optical, magnetic and structural properties which can be utilized as contrast agents for deep tissue imaging. Nie *et al.* and Gao *et al.* have designed some multifunctional nanoparticles based on semiconductor QDs for imaging and cancer treatment. For example, they encapsulated QDs with triblock copolymers for optical imaging and conjugated with targeting ligands for anticancer drug delivery (Fig. 4).[41,42] However, as contrast agents, the toxicity of QDs for human body is the most rigorous problem for clinical applications.

Since the synthesis of gold nanoparticles with tunable sizes in 1973,[43] gold-based nanostructures, including nanoshells, nanocages, nanorods, and nanostars (Fig. 5a), have always been a hot topic in optical imaging due to their tunable size for enhanced permeability and retention (EPR) effects,[2] facile surface chemistry, unique optical/electronic properties, biocompatibility and localized surface plasmon resonance (LSPR) *etc.* (Fig. 5b). Halas's group has directly compared the fluorescence enhancement by gold nanoshells and nanorods in NIR region. Their measurement revealed both nanoshells and nanorods were capable of increasing greatly the quantum yield as fluorophores, which showed tremendous potential as contrast agents for optical bioimaging.[44] Most importantly, all of the previously discussed benefits of gold nanostructures can be combined in a single vector, allowing simultaneous targeting, diagnostic and therapeutic functionality which can be chemically tailored for a particular patient or disease.[38,45] This will be illustrated in the next section in detail.

Therefore, as a safer technique, optical imaging is one of the most rapidly developing fields which nanotechnology is currently eager to combine. Along with the continuing improvement in the physical and biological properties of nanomaterials, this will bring great advantages for human health.

2.5. Ultrasound imaging

In clinical practice, US imaging is a mature technology to some extent because it has a well-established role in disease diagnosis.

The US modality, which is relatively cheap and highly patient-friendly, utilizes high-frequency sound waves usually between 1 and 40 MHz, to transmit skin and reflect back from the internal organs, reconstructing images of scanned areas. Furthermore, ultrasound allows an easy accessible, accurate, fast and real-time injection of drugs and other substances into various organs of humans or animals. However, US imaging does not allow a whole-body assessment and it is limited in imaging osseous structures or gas-containing organs such as the lungs. Innovations providing better accuracy and three-dimensional imaging approaches are currently under development and will make US a more powerful imaging strategy in the future.

In order to improve the image quality, some contrast agents can be introduced based on different acoustic properties between them and scanned tissues. The most common one is gas-containing micro-bubbles (diameters is usually between 1 and 6 μm), because of high curvature in air–liquid interfaces which can increase the intensity of the backscattered signal and enhance the echo effect.[46] In addition, functional contrast agents with specific molecules (antibodies, peptides or proteins) make ultrasound imaging able capable to identify some initially undetectable molecules and localize in a specific area of interest. Beyond micro-bubbles, nanosized bubble contrast agents (ranging in size between 10 and 1000 nm) also attract considerable interest for US imaging. Their uniform sizes promote long circulation times and accumulation in abnormal tissues. In recent decades, liposomes,[47] polylactic nanobubbles,[48,49] and solid particles like silica[50] and iron oxide particles[51] *etc.* made imaging for cancer possible when exposed to ultrasound. Kwon *et al.* reported gas-generating polymer nanoparticles (GGPNP), which encapsulate a gas precursor into polymeric nanoparticles to generate nanobubbles for US imaging after localizing in tumor (Fig. 6). From TEM images, these nanoparticles showed increased size and rapidly produced a large number of microbubbles on the surface after incubation. The results also demonstrated the feasibility of using GGPNP as US contrast agents *in vivo*.[52]

Ongoing improvements in ultrasound technology and contrast agent design will expand the clinical role of US imaging for cancer diagnosis.

3. Multimodal imaging

As mentioned above, each imaging modality has certain advantages as well as limitations, and the choice for an imaging modality, or combination of techniques, is determined by the specific biological questions being asked. In general, different imaging techniques are more complementary than competitive. They allows the detection of pathophysiological changes in early disease phases at high spatial resolution by combining the strengths of morphological/anatomical and molecular imaging modalities (for example, PET-CT and PET-MRI technology).[53–55] These technologies may change the current primarily technology-driven approach of diagnostic imaging into a more disease-oriented approach for both basic research and clinical application.

Therefore, multimodal imaging techniques, combining different imaging methods in the form of "Two-in-One" or "Multiple-in-One", will be a powerful strategy to improve the
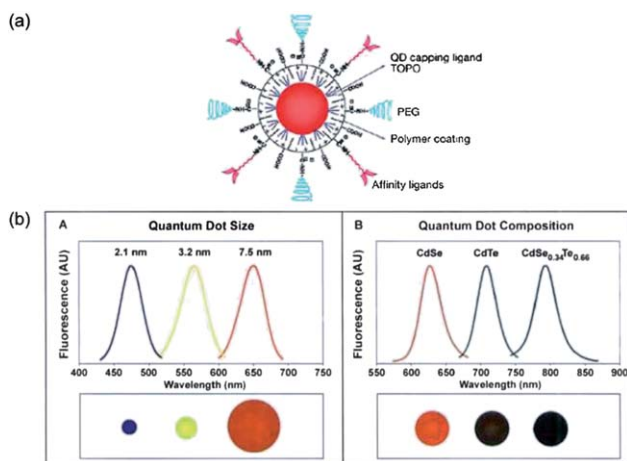

Fig. 4 (a) Scheme showing multifunctional QDs for combined *in vivo* imaging and cancer targeting; (b) the changes of the emission wavelength by varying size and composition of CdSe and CdSeTe QDs.[41,42]
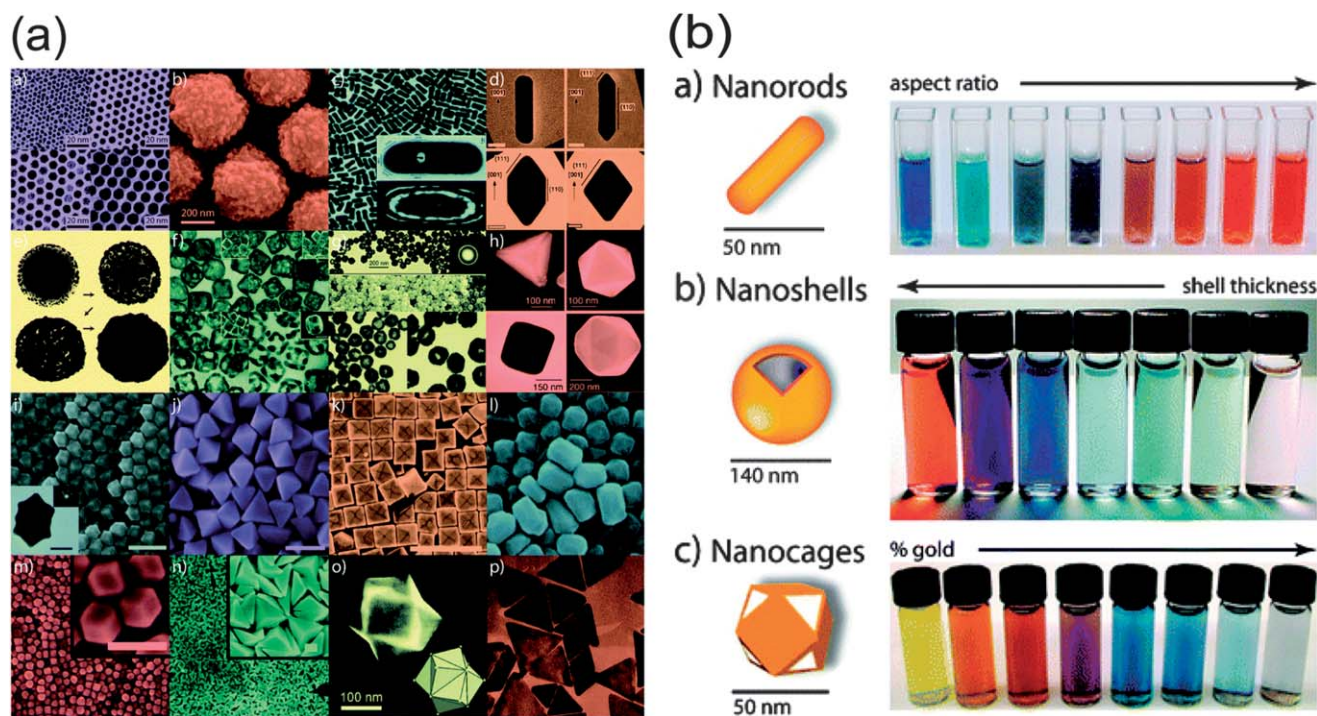
Fig. 5 (a) Various gold nanostructures with potential biomedical applications; (b) the color changes along with the aspect ratio, shell thickness and/or galvanic displacement of these gold-based nanostructures.[45]
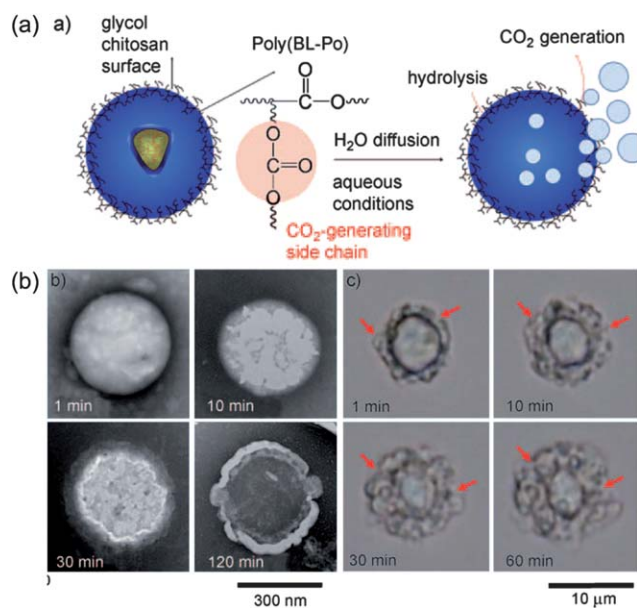

Fig. 6 (a) Schematic illustration of gas-generating polymeric nanobubbles for US imaging; (b) TEM images for these nanobubbles in different incubation times at 37 °C.[52]

imaging quality. In this section, we will discuss some increasingly popular multimodal techniques in recent years.

3.1. Photoacoustic imaging

Enormous amounts of research has applied US or optical imaging in an attempt to achieve non-invasive real-time imaging

with high resolution and sensitivity. For example, encapsulation of fluorescent probes into micro/nano-particles it is a common method to realize the modalities of US and optical imaging. However, we would like to focus on a new and promising branch of US/optical modalities – photoacoustic imaging, a hybrid biomedical imaging modality. Photoacoustic imaging is highly developed on the basis of the photoacoustic effect, which is a part of the energy from non-ionizing laser pulses that is absorbed by biological tissues and converted into heat, subsequently resulting in wideband ultrasonic waves because of transient thermoelastic expansion.[56] In photoacoustic imaging, the generated ultrasonic waves can be detected to form ultrasonic images.[57] During the past decade, photoacoustic imaging has proven to be a powerful way for visualizing biological structures and functions with prominent contrast, spatial resolution and penetration depth, overcoming the disadvantages of pure optical imaging or US.[58–60] Therefore, photoacoustic imaging is increasingly developed in the improvement of instrumentation and contrast agents.

Apart from the advances in imaging instrumentation, exogenous contrast agents can also be used to enhance the photoacoustic imaging. One of the most important factors to fabricate photoacoustic contrast agents is the ability to convert absorbed light into heat to produce ultrasound waves. Huge amounts of metal/semiconductor materials possess this function, such as silver, gold, carbon, quantum dots and so on. By reconstructing the composition, size, shape and optical properties, these structures have great potential in the detection and imaging of cancerous tissue as distinguished from healthy tissue.

Gold-based nanostructures are one of the most attractive and promising materials for photoacoustic contrast agents, because of the strong localized surface plasmon resonance (LSPR) which

can strongly convert the absorbed light into vibrational energy (heat). Moreover, the surface of gold is relatively inert, which is the main reason for its biocompatibility in *in vivo* studies. Nowadays, gold nanostructures of various shapes and sizes as mentioned above (Section 2.4.) could also be used for photoacoustic imaging): hollow gold nanospheres in Li's group;[61] gold nanocages in Xia's group;[62] and gold nanorods in El-sayed's group.[63] In Li's group, they constructed PEG conjugated-hollow gold nanospheres (PEG-HAuNS) simultaneously with optical and ultrasound properties as photoacoustic contrast agents. This nanostructure showed no acute toxicity in various organs and admirable properties in spatial resolution and sensitivity for photoacoustic imaging.[61]

Among the noble metals, silver, the same as gold, also exhibits surface plasmon resonance in exposure to laser light in the visible to NIR range. Theoretically, silver is a better photoacoustic contrast agent over gold on account of the slightly stronger light absorption. Based on this hypothesis, silver nanocages broadly absorbing NIR light were tested as photoacoustic and ultrasound imaging contrasts.[64,65] The results confirmed that the obtained images clearly visualized the location of silver nanocages *in vivo* with low background. However, even though many studies indicated that silver possessed stronger capabilities as a photoacoustic contrast agent than gold, it was more reactive and cytotoxic *in vivo*. Thus, the use of silver in biomedicine needs further studies to ameliorate the biocompatibility and stability.

Furthermore, carbon nanotubes have also shown promise as contrast agents for photoacoustic imaging of tumors and infections because they offer high resolution and allow deep tissue imaging. Gambhir's group fabricated single-walled carbon nanotubes conjugated with a cyclic Arg-Gly-Asp (RGD) peptide as targeting contrast agents for photoacoustic imaging of tumors, which showed more intensive accumulation in tumors compared with QD-RGD.[66] In order to enhance the NIR absorption to offer high resolution and deep tissue imaging, Kim *et al.* synthesized antibody-conjugated gold-plated carbon nanotubes as NIR photoacoustic contrast agents (Fig. 7).[67] These antibody-conjugated gold carbon nanotubes could map the target receptor with minimal toxicity, showing potential as an effective candidate for non-invasive targeted photoacoustic imaging *in vivo*.

The advancements in nanoscale contrast agents pave the way for application of photoacoustic imaging in real clinics. By employing nanoparticles conjugated to bioactive molecules such as proteins, antibodies and ligands, this technique will potentially be applied to the accurate noninvasive detection of tumors *in situ* with specific accumulation.

3.2. MRI/optical dual-modal imaging

MRI/optical dual imaging contrast agents have drawn intense attention because they combine the high spatial and temporal resolution of the former and the sensitivity of the latter. Based on the advances of both MRI and optical imaging, MRI/optical dual-imaging has attracted tremendous attention. In order to construct a single integrated contrast, many kinds of nanomaterials with combined functions in MRI and optical imaging have been synthesized and confirmed.
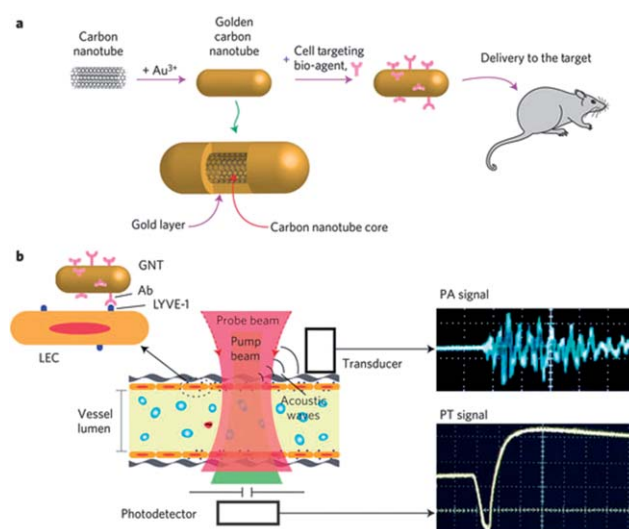

Fig. 7 Illustration of gold–carbon nanotube for photoacoustic and photothermal diagnosis and therapy.[67]

One main way to construct an MRI/optical contrast agent is to coat the surface of magnetic particles with gold. Au and Fe are not compatible with each other because of their different surface crystal structures. Thus, the most reported relative studies always use some dielectric materials as an intermediate layer between the gold and magnetic core. The most common materials are silica,[68] polymers,[69] liposomes[70] and so on, which greatly promote the synthesis of composite nanomaterials. Shi *et al.* reported combined MRI and optical imaging by simply coating optically active plasmonic components (*e.g.* Au) on the magnetic component. With positive silica as a media, the synthesized magnetic-gold core–shell nanostructure simultaneously achieved strong T_2-weighted relaxation and high NIR light absorption around 800 nm (Fig. 8).[68] Moreover, some gold nanostructures such as gold nanorods and nanostars have high absorption in the NIR window. As a result, fabricating this kind of structure with gold as a core for optical imaging and iron oxide outside for MRI is also a feasible way to achieve MRI/optical dual-modal imaging. For instance, Murphy *et al.* tried to form uniform
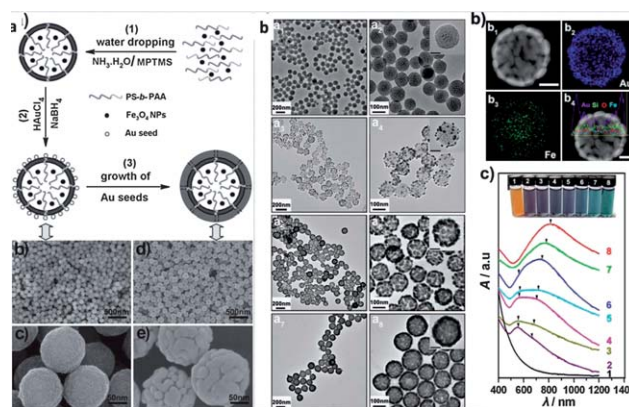

Fig. 8 (a) Scheme of fabrication of Fe_3O_4@hybrid@Au nanoparticles; (b) TEM images and UV-vis-NIR spectra of nanostructure in different procedures.[68]

coatings of iron oxide nanoparticles onto the surface of gold nanorods for potential multifunction imaging.[71]

As mentioned above, QDs can also supply excellent fluorescent properties for optical imaging, so the combination of QDs and magnetic nanomaterials is another potential candidate for MRI/optical dual-mode imaging. Hyun *et al.* provided an easy strategy to fabricate multimodal imaging nanoprobes for both MRI and NIR imaging.[72] In their study the MRI contrast agents, $MnFe_2O_4$ nanoparticles, were encapsulated in the ionic nanocomplex. Subsequently, NIR-emitting fluorescent QDs were assembled on the surface through electrostatic absorption. The final nanostructures showed high efficiency for MR/NIR dual-modality imaging in cancer detection.

Based on the development of NIR dyes, this is an easy and feasible way to modify MRI contrast agents with dyes for optical imaging.[73] With simple chemical/physical modification, extant MRI contrast agents will achieve good ability for NIR optical imaging without damaging the MRI imaging signals. For example, Medarova and colleagues developed NIR dye-labeled SPIONs for simultaneous MRI and NIR optical imaging. The acquired imaging nanoparticles had a strong T_2-weighting, showing multifunctional imaging and high intensity of the NIR signal in the tumors.

As a result, MRI/optical dual imaging has proved to be practically feasible by many studies in current years. However, it is still challenging to engineer systematically reliable coatings for these nanoparticles capable of promoting favorable interactions with the biological system for *in vivo* applications.

3.3. US/MRI dual-modal imaging

Currently, US and MRI imaging are performed clinically as separate examinations, typically on different days, with the subject in a different orientation. To improve both temporal and spatial accuracy, accurate US/MRI dual-modal imaging is required.[74] The feasibility of US/MRI dual-modalities has been successfully demonstrated. Some studies indicated that US/MRI systems could provide benefits to better classify tissue/tumor and additionally provide complementary vascular information.[75,76]

The dual-mode contrast agents for simultaneous MRI and US imaging are mostly based on the existing US contrast media. According to previous studies, microbubbles and nanobubbles for US imaging could encapsulate or absorb MRI contrast agents to achieve MRI/US dual-imaging. Protein-shell microspheres filled with iron oxide nanoparticles,[77] stable nano-emulsion droplets containing fluorine (^{19}F) MRI contrasts[78] and iron oxide nanoparticle-embedded polymeric microbubbles[79] have been proved as dual-modal contrast agents with efficient imaging properties.

Moreover, some metal nanoparticles can also be reconstructed as dual-imaging contrast agents. Gao *et al.* prepared gold-coated iron oxide nanoparticles with well-defined core–shell structural characteristics.[70] This gold component in the nanocomposites enabled conventional photoacoustic imaging and the iron oxide component could respond to an external magnetic field for background elimination, this was called magnetomotive photoacoustic imaging. This new modality had a remarkably enhanced signal-to-noise ratio compared with conventional approaches.

Conclusively, as an imaging method of high-quality, state-of-the-art, convenience and low-cost, US-based multimodal imaging is increasingly attractive for the development of novel and smart imaging systems.

3.4. Triple-modal imaging

Except for the dual-imaging, some groups also did researches on the development of triple-multimodal imaging. They focused on combining three different imaging probes into a single hybrid probe to obtain simultaneously high sensitivity, real-time and detailed 3D anatomical information.

For example, Park *et al.* fabricated ^{124}I-labeled thermally cross-linked superparamagnetic iron oxide nanoparticles as a triple-modality probe of optical/PET/MR imaging.[80] Therefore, optical imaging was shown to be achieved using Cerenkov light emitted from the radionuclides ^{124}I, used clinically for PET imaging. The results (Fig. 9) indicated minimal background and anatomical information with PET imaging, accurate visualization of the activity distribution in the internal organs with optical imaging, and detailed tomographic anatomical information with MRI, which were consistent with the *in vivo* imaging results.

Shi's group reported a trimodal imaging probe constructed by a core–shell sub-50 nm multifunctional nanoparticle which was technically challenging for combining fluorescence, CT and MR imagings. These as-designed nanoprobes displayed strong emissions for optical imaging, short T_1 relaxation time for MRI and an enhanced Hounsfield unit (HU) value for CT.[81] However, there are still some drawbacks, such as that the nanoprobes were injected locally in the tumor, needing much greater improvement for real clinical use. In order to extend the circulation time, Saatchi *et al.* used the tested high molecular weight HPG with biocompatibility and long-circulating plasma half-life to construct a novel trimodal imaging agent for combined SPECT, MR and optical imaging.[82]

With this imaging information, it is useful in preclinical investigations to yield highly specific and quantitative data regarding tumor behavior *in vivo*. Along with advances in nanomaterials and engineering, the triple-modal imaging technique may bring a new era for preclinical and clinical diagnosis.
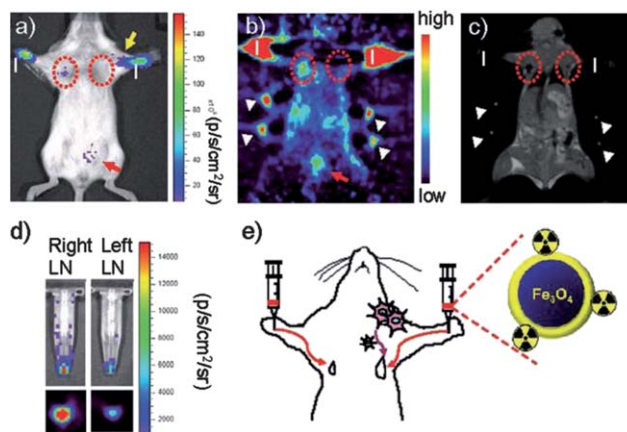

Fig. 9 Triple-modality nanoprobe for simultaneous optical/PET/MRI imaging tumor metastasis model and injection route of radio-labeled nanoparticles.[80]

4. Imaging-guided cancer therapy

With the development of nanotechnology and materials science, enormous nanomaterials have been studied for cancer treatment, such as liposomes, micelles, polymers, noble metal nanoparticles, semiconductor materials, carbon nanotubes, fullerenes, magnetic nanoparticles and metal–organic frameworks (MOFs) etc.[83] Most nano-systems for delivery of chemotherapeutic agents rely on their own special functions such as EPR effects, pH/redox/temperature-sensitivity, enzymatic responsiveness, and recognition moieties. However, those kinds of nano-systems still could not target tumor sites efficiently considering the fact that cancers are immensely heterogeneous and all existing treatments are effective for only limited patient subpopulations and at selective stages of diseases development.[84] However, imaging-guided therapy is a close marriage of diagnosis and therapy, that is "theranostic", and could provide therapeutic protocols that are more specific to individuals and, therefore, more likely to offer improved prognoses.[85] Here, we will introduce some novel therapeutic methods with imaging guidance, including hyperthermia, photothermal and photodynamic therapy, and their developing biomedical materials.

4.1. Imaging-guided magnetic hyperthermia therapy

Hyperthermia, initially named overheating, has been utilized in treatment of malignant tumors as long as medicine.[86] The heat produced by hyperthermia can raise the temperature of tumor tissue as high as 41–46 °C. According to previous reports, tumors are more easily heated and much more sensitive to temperature in the range of 42–45 °C than are normal cells, basically due to their poorer vascularization.[87,88] In addition, heat can be applied locally with no systemic effects to surrounding cells and reduced side effects compared to traditional treatments. As a result, hyperthermia currently remains a promising assisting form of cancer therapy with the established chemotherapy, radiotherapy and surgery. Unfortunately, the gap between the raised temperature by hyperthermia and that in normal tissue is too small. Therefore, hyperthermia is commonly accompanied by imaging guidance or other therapeutic modalities. Among various hyperthermia modalities, magnetically induced hyperthermia is a main branch of hyperthermia therapies for cancer treatments by exposing cancer tissues to an alternating magnetic field. This is effective because the magnetic field can be applied to deep tissues and will not be absorbed by living tissues.[89]

Based on the nature of magnetic nanoparticles, they can simultaneously contribute to imaging contrast and the heating source due to magnetic hysteresis loss.[90] As a result, heat could be generated by alternating a magnetic field to kill tumor cells as long as the imaging visualizes the location of the magnetic particles, which will efficiently reduce undesirable damage to normal tissues. The most common materials for hyperthermia are iron oxide nanoparticles. Many previous reports have demonstrated the various functions of iron oxide nanoparticles in imaging and hyperthermia. Some other elements are introduced as dopants into the iron oxide nanoparticles to improve their performance. Initially, Drake et al. reported the synthesis of Gd-doped iron oxide nanoparticles and showed that they were able to generate magnetic resonance images with higher quality

without tampering their hyperthermia effects.[91] However, researchers began to focus on more biocompatible elements, such as Zn and Mn[92] taking into accounts the toxicity of Gd. For example, Zn and Mn ion doped iron oxide nanoparticles $(Zn_{0.4}Mn_{0.6})Fe_2O_4$ seem to be promising candidates for hyperthermia, able to kill 84.4% of HeLa cells within 10 min after the application of the AC magnetic field, and simultaneously show higher potential as MRI contrast agents over conventional iron oxide (Fig. 10).[93]

Additionally, the target moiety for magnetic nanoparticles is also a prominent aspect in the design of these nanosystems. With the guidance of a targeting ligand, magnetic nanoparticles could positively accumulate in cancer tissues and subsequently kill tumorous cells by hyperthermia. Various ligands, including folic acid,[94] epidermal growth factor receptor (EGFR),[95] and antibodies,[96] have been applied to the surface of magnetic nanoparticles with physical or chemical methods.

Moreover, the heat from magnetic-field-induced hyperthermia can also be manipulated as stimulus to combined therapy. As mentioned above, magnetic nanoparticles with uniform size can be synthesized in a well-controlled manner. For mesoporous materials, the small-size magnetic nanoparticles can be used as a cap to control drug release. Lin's group reported superparamagnetic iron oxide nanoparticle capped mesoporous silica nanocarriers which are controllable for drug release under an external magnetic field (Fig. 11).[97] Furthermore, nanoparticles with a magnetic core are equally attractive for combined therapy
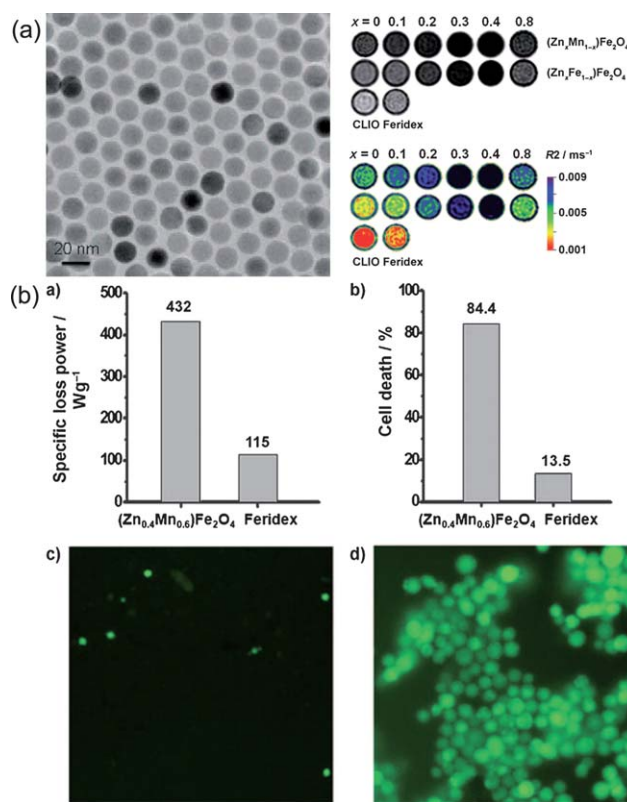

Fig. 10 (a) TEM images and MRI contrast effects of 15 nm $(Zn_{0.4}Mn_{0.6})Fe_2O_4$ nanoparticles; (b) the hyperthermia caused by $(Zn_{0.4}Mn_{0.6})Fe_2O_4$ nanoparticles can kill most HeLa cells.[93]

under magnetic stimulation. Baeza *et al.* constructed thermo-responsive copolymer poly(ethyleneimine)-*b*-poly(*N*-iso-propylacrylamide) (PEI/NIPAM) on the surface of mesoporous silica nanoparticles with encapsulated iron oxide.[98] When the magnetic field is alternating, the rising temperature triggers the release of therapeutic agents as chemotherapy, along with hyperthermia and MRI. This device confirmed the excellent promise of combination of imaging-guided hyperthermia and conventional chemotherapy.

Based on these examples, imaging-guided hyperthermia holds great promise to visualize treatment procedures in combination with other therapeutic methods.

4.2. Imaging-guided photothermal therapy

Besides magnetic-induced hyperthermia, light can also be used in heating as a cancer treatment, which is called "photothermal" therapy. Particularly, for noble metal nanocrystals, their localized surface plasmon resonance (LSPR) leads them to absorb NIR light and convert it into vibrational energy (heat). As in magnetic hyperthermia, the heat produced by the photothermal effect provides an attractive external input to actuate photothermal therapy to specifically kill cancerous cells and inhibit tumor growth.

For example, specially tailored gold nanostructures with absorbing peaks in the NIR regions, such as gold nanorods, nanoshells and nanocages have shown considerable efficacy for tumor ablation under NIR light irradiation, which highlights their clinical promise and also motivates the further development of photothermal therapies. In Bhatia's research, gold nanorods protected by polyethylene glycol (PEG) (PEG-NRs) exhibited an outstanding spectral bandwidth, photothermal heat generation per gram of gold and long circulation half-life *in vivo*. The results indicated that they possessed approximately two times higher absorption of 810 nm light than clinical iodine contrast agents and high accumulation at the tumor area 72 hours after injection (Fig. 12).[99] In Tang's research, multifunctional gold nanoshells

on silica nanorattles exhibited a high absorption intensity of 800 nm light in NIR spectrum and a prominent ability to generate heat, allowing the combination of photothermal therapy and imaging.[100] Liu and co-workers synthesized gold-nanoshelled microcapsules for US imaging and photothermal therapy.[101] As their results demonstrated, the bubbles in the microcapsules could enhance the US imaging in a latex tube; and those nanostructures have a high absorption in the NIR region, which have potential as optical imaging contrast agents, even though they were used for photothermal therapy in this paper.

On the other hand, the heat of photothermal effect also can be used as a trigger for combined therapy on the basis of imaging guidance. Xia *et al.* constructed a controlled-release system by using temperature-sensitive polymer (pNIPAAm) coated Au nanocages. The rise in temperature after exposure to NIR lasers caused the polymer chains to collapse, and therefore release the pre-loaded drugs/dyes (Fig. 13).[102] This inspires us to actively control the therapeutic agents' behavior on the precondition of direct imaging confirmation, which will pave the advance of real specific treatment for personalized medicine.

Moreover, Bhatia *et al.* constructed nanosystems consisting of signaling molecules and receiving modules by taking inspiration from swarming. The gold nanorods acted as the former to generate heat under NIR irradiation and accelerated the recruitment of various receiving modules in the tumor. The results indicated that those systems based on the communication of diagnostic and therapeutic agents could be engineered to a more sensitive location, diagnose and treat diverse human diseases.[103,104]

Furthermore, some other nanocrystals can also induce photothermal therapy with imaging function. Dai's work, showed that ultrasmall multifunctional FeCo/graphite shell nanocrystals could be applied as a system for NIR photothermal
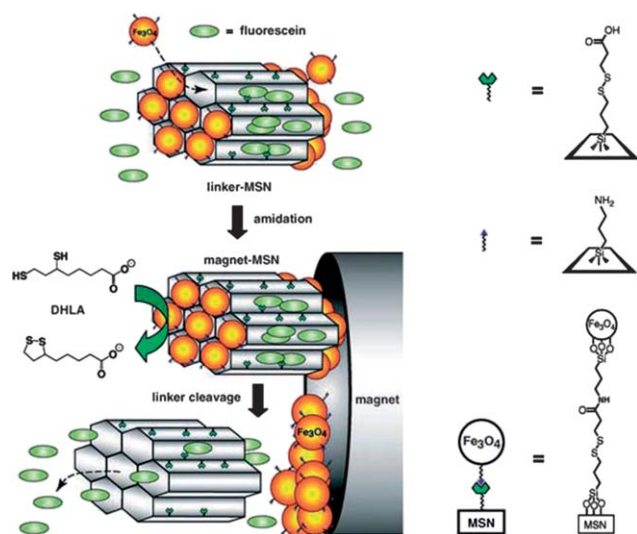

Fig. 11 Schematic of superparamagnetic iron oxide-capped mesoporous silica nanorods for stimuli-responsive drug delivery.[97]
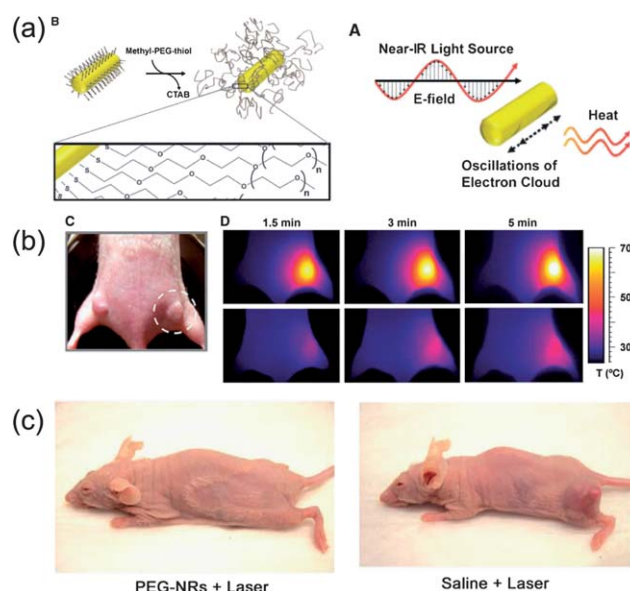

Fig. 12 (a) Scheme of coating PEG on gold nanorods' surfaces and photothermal heating of gold nanorods; (b) passive tumor targeting and photothermal heating of passively targeted gold nanorods antennas in tumors; (c) photothermal destruction of human tumors in mice using PEG-coated nanorods.[99]
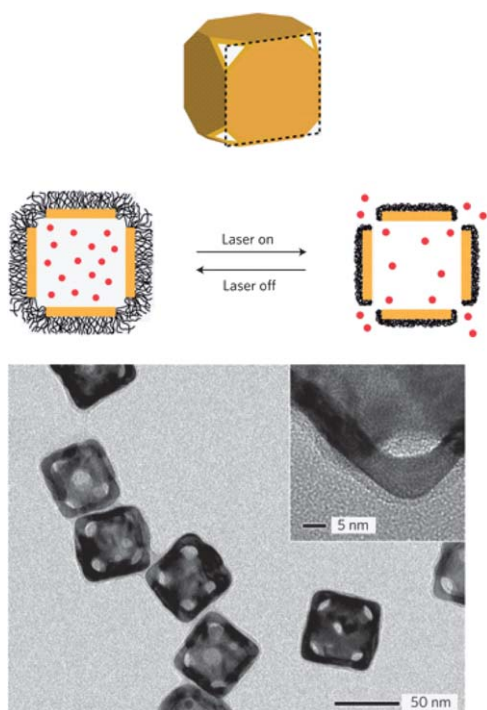
Fig. 13 Schematic illustration and characterization of the gold nanocage for controllable release.[102]

therapy and MRI *in vitro*.[105] In addition, ligand-stabilized copper selenide (Cu_2–xSe) nanocrystals exhibited strong NIR optical absorption and produced significant photothermal heating by exciting them with 800 nm light, comparable to gold nanorods and nanoshells. Cu_2–xSe nanocrystals were able to result in cell destruction only after 5 min of laser irradiation, demonstrating their prominent viability for photothermal therapy.[106]

Photothermal therapy has been confirmed as promising in the field of in cancer treatment and imaging-guided photothermal therapy will be an attractive rising method for visualized cancer therapy with advances in materials and nanotechnology. However, the penetration depth of light is still a critical issue for clinical applications. Meanwhile, potential phototoxicity in the microenvironment also needs to be investigated carefully.

4.3. Imaging-guided photodynamic therapy

Instead of killing cancer cells by inducing heat, light itself has been used as therapy for thousands years. Since the discovery that oxygen played an important role in the process of light-induced therapy,[107] many researchers found that photodynamic therapy (PDT), a combined utilization of light and a photosensitizer, has a direct destroying effect on cancer cells and the tumor vasculature. In PDT, the photosensitizer is capable of converting light into molecular oxygen and generate reactive oxygen species (ROS) to kill tumor cells and/or tissues by multiple-factor mechanisms.[108] The subsequent biological responses will only happen in the particular areas of tissue exposed to light because of the localization of the light-absorbing photosensitizer.[109] Therefore, PDT expands its promising

potential in clinical treatment for cancers with reduced side effects.

The localization of photosensitizers in tissue/cellular sites is very important in therapeutic procedures. At this point, imaging was appended as a direct guidance. Commonly, various photosensitizers are labeled with dyes, so the location of photodynamic therapeutic agents can be visualized by optical imaging. However, the fluorescence yield can vary with the binding site, so that sites of photosensitizers may not be precise enough by fluorescent imaging.[110] Additionally, most photosensitizers are excited by visible or even UV light, which has limited penetration depth and even causes biological damage. These disadvantages have promoted the next-generation of NIR light induced nano-photosensitizers, which highlights the promise for multifunctional *in vivo* cancer imaging and treatment.

One of the approaches to integrate photodynamic therapy and imaging is to synthesize NIR-light absorbed photosensitive molecules. A previous study reported a way to synthesize FeL-(cat)(NO_3) complex as a PDT agent activated by NIR light as a cellular fluorophore. The results indicated that this iron(III) complex had significant NIR-light-induced photocytotoxicity and negligible dark toxicity.[111] Moreover, based on the ability for NIR fluorescence imaging of some special nanostructures, it is feasible to combine photosensitizers with NIR imaging contrast agents. Gold-based nanomaterials have outstanding qualities for optical imaging and photothermal therapy as described in Imaging-guided cancer therapy section. While combined with photosensitive agents, these gold nanostructures attracted more attention for multiple biological applications. Recently, Choi's group introduced a multifunctional nanomedicine platform consisting of gold nanorods and a photosensitizer $AlPcS_4$ for both non-invasive imaging and photodynamic cancer therapy. With this system, tumor sites could be visualized by NIR fluorescence imaging, and subsequently highly effective dual photothermal and photodynamic therapy was induced (Fig. 14).[112] NIR light excited upconversion nanoparticles (UCNPs) showed various benefits including reduced autofluorescence background, improved tissue penetration depth and enhanced photostability for imaging. Wang *et al.* constructed photosensitizer Chlorin e6(Ce6) conjugated UCNPs for imaging-guided therapy (Fig. 15).[113] Some other nanomaterials also have been demonstrated as carriers for photodynamic agents, including mesoporous silica nanoparticles,[114] nanocapsules,[115] semiconductor
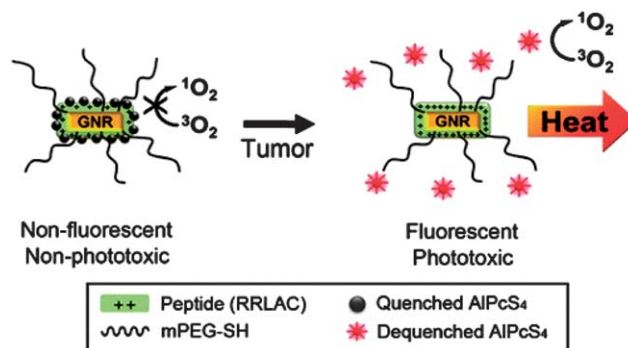

Fig. 14 Schematic diagram of the gold nanorods conjugated with $AlPcS_4$ for simultaneous NIR optical imaging and phototherapy.[112]
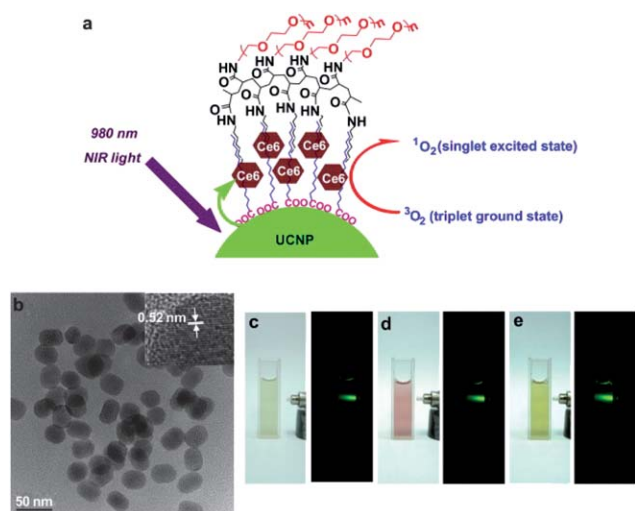
Fig. 15 Scheme of loaded-Ce6 PEGylated UCNPs for optical imaging-guided photodynamic therapy.[113]

quantum dots[116] and so on. All those materials also showed strong potential for photodynamic cancer therapy.

PDT has been used in oncology for more than 25 years, but it still cannot replace conventional therapy even if it had much lesser side effects. To date, most photosensitizers were developed for cancer treatment only based on their chemical and physical qualities to improve the optical properties, rather than biological or clinical capabilities. Modification of a sensitive moiety through its physicochemical properties or improved targeting by conjugation of the photosensitizer to moieties such as antibodies, polymers and peptide scaffolds, might overcome the present difficulties. In particular, combining imaging methods can provide photodynamic therapy a visual guide and controllable target, which will ensure a substantial future role for this type of treatment in oncology.

4.4. Imaging-guided surgery

For clinical cancer therapy, operative resection is an inevitable and most common procedure for the treatment of tumors. From the early eighteenth century, imaging-guided surgery became one of the main methods of clinical treatment. Before surgery, physicians always need to draft a plan based on possible overall diagnosis results, especially imaging results. Imaging results provide the information about size, shape and location which are critical to the success of surgery. However, currently existing imaging techniques have their own limitations which probably bring more danger into the treatment. For example, MRI can indicate the size, shape and location of a tumor, but all these items of information are not enough to confirm precisely the fine margin between tumor and normal tissue, as well as the depth of a tumor in the human body. Additionally, physicians cannot resect all tumor tissue because of its indistinct margin, which increases the possibility of recrudescence of the cancer. Therefore, it has becoming increasingly crucial to develop contrast agents to achieve extremely precise imaging.

Nanotechnology provides a beneficial stage for novel imaging contrast agents, considering the distinct physical/chemical properties of nanomaterials. Except as imaging contrast agents themselves, nano-materials can integrate multiple functions into one platform to achieve better diagnosis and imaging. Gambhir's group reported a novel triple-modality nanoparticle for molecular imaging to guide every step of surgery for brain tumors as Fig. 16. Gd-DOTA, the MRI contrast, was modified on the surface of nanoparticles to provide primary information for surgery planning; the Raman active layer between the silica-shell and gold-core could visualize the fine margin of the tumor to allow accurate resection during surgery, and also be used as confirmation of clean margins *ex vivo* after surgery; the 60 nm gold-core could enhance Raman signal due to the surface plasmon resonance and also be used to photoacoustic imaging for detecting deep tumors under normal tissue. Their results indicated that this kind of triple-modality nanoparticle could specially recognize tumor cells and visualize the boundary, and the resection of tumor was much cleaner with the help of this imaging. This strategy was designed for whole brain tumor surgery, which brings in more accurate diagnosis, cleaner resection and lower possibility of recurrence.[117] Olson *et al.* also reported an imaging-guided surgery strategy based on multifunctional nanoparticles. In their system, gadolinium was labeled on dendrimeric nanoparticles as a long-lasting MRI contrast to provide diagnostic information and presurgical planning; the fluorescent molecule Cy5 was also used as a label for intraoperative fluorescence-guided surgery.[118]

Thus, integrating nanotechnology-based imaging with clinical operative is one promising way to improve efficiency of cancer therapy. Many researchers have demonstrated the possibility of imaging-guided surgery, but there are still many urgent issues that need to be solved or improved. For example, the long circulation time of nanoparticles in the blood will be fit for clinical presurgical preparation and the accuracy of operative planning; special targeting to the tumor will maximally reduce side effects on normal tissues; a high time/spatial resolution of imaging will provide more distinct information on the tumor which benefit physicians to deal with any problems during surgery. With those issues solved, imaging-guided surgery will bring in a new era for cancer therapy.
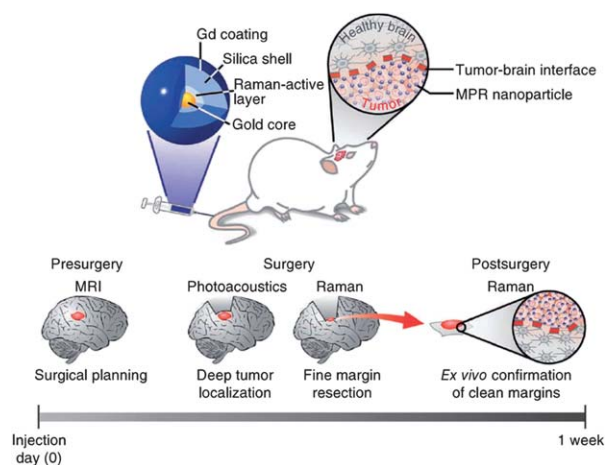

Fig. 16 Triple-modality MRI–photoacoustic–Raman imaging strategy for entire brain tumor surgery.[117]

5. Summary and perspective

In this review, we have shown the possibilities to create different nanoobjects as imaging contrast agents and therapeutic media. The approach of using nanomaterials for specific targeting, molecular imaging and selective therapy is both general and versatile. The general paradigm of this research area has been well-established: synthesis, functionalization, characterization and performance evaluation. Nanomaterials with special optical, electrical and magnetic properties make it possible for us to diagnose and treat cancer in more than one way. Those "two-in-one" or "multiple-in-one" modalities make personalized and integrated therapy feasible. Based on the imaging visualization and diagnosis, the therapeutic schedule will be designed more accurately and personally. As a result, the cooperative therapeutic agents and intrinsic function will be activated to kill cancer locally with minimal side effects. After that, the imaging can also be utilized for re-examination. Thus, with these nanomaterials, the normal complicated disease treatments in hospital, including diagnosis, detection, therapy and re-examination, are integrated into a single personal way, which greatly simplifies the treatment, decreases the side effect and lowers the cost for patients.

The ultimate goal for this research field is to re-shape cancer treatment at the clinical level. However, there are still three problems for pushing the utilization of nanomaterials into real clinical applications. Firstly, the design and fabrication of these nanoscale agents are quite arbitrary. Researchers have not had a set of rules to choose materials that perfectly meet the needs; Secondly, the mechanism of nanotoxicity has not been fully understood and nanostructures have not been trusted for in vivo applications. In past few years, many researchers have pointed out the potential toxicity of nanomaterials in in vivo application. For instance, surface charge,[119] ligands,[120] size,[121] shape,[122] even different cell lines[123] will result in different effects to microenvironment. Especially, size-dependent toxicity is one of the most critical issues. According to previous results, the different size of nanomaterials will be subjected to different metabolism processes in vivo. Nanoparticles with sizes less than 5 nm will be easily cleared by the blood as the average pore size of the normal endothelium is around 5 nm; those with sizes more than 100 nm prefer to accumulate in liver, kidney, spleen and lung because of the MPS (mononuclear phagocyte system); those with sizes around 50 nm are widely applied in priority as nanomedicine because they are generally considered to have less toxicity and favourable biodistribution and clearance/accumulation behavior.[124–126] Thirdly, the metabolism of nanomaterials should be further studied in detail. As mentioned above, the accumulation of nanomaterials in the RES organs is potentially harmful to human bodies. Especially, for those nanomaterials which cannot be degraded or removed by the microenvironment, the higher accumulation their in the RES organs, the higher the possibility that they will do harm to human bodies. Moreover, the metabolic pathway of nanomaterials is still not fully biologically understood. The receptor-mediated endocytosis processes that nanomaterials are subjected to, the signaling proteins that nanomaterial activate, and so on are mysteries which make it much more difficult to control the behavior of nanostructures.

The development of biomedical nanomaterial-based cancer imaging and therapy has continuously involved cross-background researchers, such as biologists, pathologists, chemists, material scientists, doctors and engineers. Rapid progress in interdisciplinary research may help out with these problems. For example, materials scientists and chemists will offer more novel material candidates for potential application; pathologists will investigate how size and surface ligands influence the toxicity of nanomaterials and then optimize for minimization of the side effect. We believe that nanomaterial-based cancer imaging and therapy will help us envision the era of personalized medicine. Patients with cancer can be truly subjected to treatment that is designed to the specific individual, and the opportunity for recovery of a patient from deadly disease will finally come in the foreseeable future.

Acknowledgements

Notes and references

1 X. Chen, S. S. Gambhir and J. Cheon, *Acc. Chem. Res.*, 2011, **44**, 841.
2 R. K. Jain and T. Stylianopoulos, *Nat. Rev. Clin. Oncol.*, 2010, **7**, 653–664.
3 T. C. Lai, Y. Bae, T. Yoshida, K. Kataoka and G. S. Kwon, *Pharm. Res.*, 2010, **27**, 2260–2273.
4 G. Helmlinger, F. Yuan, M. Dellian and R. K. Jain, *Nat. Med.*, 1997, **3**, 177–182.
5 M. Mahmoudi, V. Serpooshan and S. Laurent, *Nanoscale*, 2011, **3**, 3007–3026.
6 J. K. Willmann, N. van Bruggen, L. M. Dinkelborg and S. S. Gambhir, *Nat. Rev. Drug Discovery*, 2008, **7**, 591–607.
7 C. W. Park, Y. S. Rhee, F. G. Vogt, D. Hayes Jr, J. Zwischenberger, P. P. DeLuca and H. M. Mansour, *Adv. Drug Delivery Rev.*, 2012, **64**, 344–356.
8 M. Dolovich and R. Labiris, *Proc. Am. Thorac. Soc.*, 2004, **1**, 329–337.
9 R. Weissleder and U. Mahmood, *Radiology*, 2001, **219**, 316–333.
10 J. C. Miller and J. H. Thrall, *J. Am. Coll. Radiol.*, 2004, **1**, 4–23.
11 J. C. Miller and J. H. Thrall, *J. Am. Coll. Radiol.*, 2004, **1**, 4–23; D. J. Brenner and E. J. Hall, *N. Engl. J. Med.*, 2007, **357**, 2277–2284.
12 S. S. Gambhir, *Nat. Rev. Cancer*, 2002, **2**, 683–693.
13 M. Tubiana, *N. Engl. J. Med.*, 2008, **358**, 850.
14 R. Popovtzer, A. Agrawal, N. A. Kotov, A. Popovtzer, J. Balter, T. E. Carey and R. Kopelman, *Nano Lett.*, 2008, **8**, 4593–4596.
15 D. Kim, S. Park, J. H. Lee, Y. Y. Jeong and S. Jon, *J. Am. Chem. Soc.*, 2007, **129**, 7661–7665.
16 A. Miyamoto, H. Okimoto, H. Shinohara and Y. Shibamoto, *Eur. Radiol.*, 2005, **16**, 1050–1053.
17 M. G. Harisinghani, J. Barentsz, P. F. Hahn, W. M. Deserno, S. Tabatabaei, C. H. van de Kaa, J. de la Rosette and R. Weissleder, *N. Engl. J. Med.*, 2003, **348**, 2491–2499.
18 O. Veiseh, J. W. Gunn and M. Zhang, *Adv. Drug Delivery Rev.*, 2010, **62**, 284–304.
19 T. Tamada, K. Ito, T. Sone, A. Yamamoto, K. Yoshida, K. Kakuba, D. Tanimoto, H. Higashi and T. Yamashita, *J. Magn. Reson. Imaging*, 2009, **29**, 636–640.
20 J. Park, K. An, Y. Hwang, J. G. Park, H. J. Noh, J. Y. Kim, J. H. Park, N. M. Hwang and T. Hyeon, *Nat. Mater.*, 2004, **3**, 891–895.
21 Y. Jun, Y. M. Huh, J. Choi, J. H. Lee, H. T. Song, S. Kim, S. Yoon, K. S. Kim and J. S. Shin, *J. Am. Chem. Soc.*, 2005, **127**, 5732–5733.

22 D. L. J. Thorek, A. K. Chen, J. Czupryna and A. Tsourkas, *Ann. Biomed. Eng.*, 2006, **34**, 23–38.

23 B. H. Kim, N. Lee, H. Kim, K. An, Y. I. Park, Y. Choi, K. Shin, Y. Lee, S. G. Kwon, H. B. Na, J. Park, T. Ahn, Y. Kim, W. K. Moon, S. H. Choi and T. Hyeon, *J. Am. Chem. Soc.*, 2011, **133**, 12624–12631.

24 A. J. Rondinone, A. C. S. Samia and Z. J. Zhang, *J. Phys. Chem. B*, 1999, **103**, 6876–6880.

25 C. Khemtong, O. Togao, J. Ren, C. W. Kessinger, M. Takahashi, A. D. Sherry and J. Gao, *J. Magn. Reson.*, 2011, **209**, 53–60.

26 H. B. Na, I. C. Song and T. Hyeon, *Adv. Mater.*, 2009, **21**, 2133–2148.

27 L. Zhou, Z. Gu, X. Liu, W. Yin, G. Tian, L. Yan, S. Jin, W. Ren, G. Xing and W. Li, *J. Mater. Chem.*, 2012, **22**, 966–974.

28 Y. I. Park, J. H. Kim, K. T. Lee, K. S. Jeon, H. B. Na, J. H. Yu, H. M. Kim, N. Lee, S. H. Choi and S. I. Baik, *Adv. Mater.*, 2009, **21**, 4467–4471.

29 L. Zhang, M. Yin, H. You, M. Yang, Y. Song and Y. Huang, *Inorg. Chem.*, 2011, **50**, 10608–10613.

30 R. J. Xing, G. Liu, Q. M. Quan, A. Bhirde, G. F. Zhang, A. Jin, H. Bryant, A. Zhang, A. Liang, H. S. Eden, Y. L. Hou and X. Y. Chen, *Chem. Commun.*, 2011, **47**, 12152–12154.

31 K. An, S. G. Kwon, M. Park, H. B. Na, S. I. Baik, J. H. Yu, D. Kim, J. S. Son, Y. W. Kim and I. C. Song, *Nano Lett.*, 2008, **8**, 4252–4258.

32 R. T. Sadikot and T. S. Blackwell, *Proc. Am. Thorac. Soc.*, 2005, **2**, 537.

33 C. E. Badr and B. A. Tannous, *Trends Biotechnol.*, 2011, **29**, 624–633.

34 K. L. Farina, J. B. Wyckoff, J. Rivera, H. Lee, J. E. Segall, J. S. Condeelis and J. G. Jones, *Cancer Res.*, 1998, **58**, 2521–2528.

35 J. Condeelis and J. E. Segall, *Nat. Rev. Cancer*, 2003, **3**, 921–930.

36 R. M. Hoffman, *Nat. Rev. Cancer*, 2005, **5**, 796–806.

37 A. M. Smith, M. C. Mancini and S. Nie, *Nat. Nanotechnol.*, 2009, **4**, 710.

38 E. C. Dreaden, M. A. Mackey, X. Huang, B. Kang and M. A. El-Sayed, *Chem. Soc. Rev.*, 2011, **40**, 3391–3404.

39 U. Mahmood and R. Weissleder, *Mol. Cancer Ther.*, 2003, **2**, 489.

40 E. M. Sevick-Muraca, *Annu. Rev. Med.*, 2012, **63**, 217–231.

41 X. Gao, Y. Cui, R. M. Levenson, L. W. K. Chung and S. Nie, *Nat. Biotechnol.*, 2004, **22**, 969–976.

42 A. M. Smith, X. Gao and S. Nie, *Photochem. Photobiol.*, 2004, **80**, 377–385.

43 G. Frens, *Nature*, 1973, **241**, 20–22.

44 R. Bardhan, N. K. Grady, J. R. Cole, A. Joshi and N. J. Halas, *ACS Nano*, 2009, **3**, 744–752.

45 E. C. Dreaden, A. M. Alkilany, X. Huang, C. J. Murphy and M. A. El-Sayed, *Chem. Soc. Rev.*, 2012, **41**, 2740–2779.

46 S. P. Qin, C. F. Caskey and K. W. Ferrara, *Phys. Med. Biol.*, 2009, **54**, 27–57.

47 A. Yudina, M. de Smet, M. Lepetit-Coiffé, S. Langereis, L. Van Ruijssevelt, P. Smirnov, V. Bouchaud, P. Voisin, H. Grüll and C. Moonen, *J. Controlled Release*, 2011, **155**, 442–448.

48 J. S. Xu, J. W. Huang, R. G. Qin, G. H. Hinkle, S. P. Povoski, E. W. Martin and R. X. Xu, *Biomaterials*, 2010, **31**, 1716–1722.

49 C. W. Burke, Y. H. J. Hsiang, E. Alexander IV, A. L. Kilbanov and R. J. Price, *Small*, 2011, **7**, 1227–1235.

50 Y. L. Liu, Y. H. Wu, W. B. Tsai, C. C. Tsai, W. S. Chen and C. S. Wu, *Carbohydr. Polym.*, 2011, **84**, 770–774.

51 X. Cai, F. Yang and N. Gu, *Theranostics*, 2012, **2**, 103–112.

52 E. Kang, H. S. Min, J. Lee, M. H. Han, H. J. Ahn, I. C. Yoon, K. Choi, K. Kim, K. Park and I. C. Kwon, *Angew. Chem., Int. Ed.*, 2010, **49**, 524–528.

53 H. U. Gerth, K. U. Juergens, U. Dirksen, J. Gerss, O. Schober and C. Franzius, *J. Nucl. Med.*, 2007, **48**, 1932–1939.

54 M. S. Judenhofer, H. F. Wehrl, D. F. Newport, C. Catana, S. B. Siegel, M. Becker, A. Thielscher, M. Kneilling, M. P. Lichy and M. Eichner, *Nat. Med.*, 2008, **14**, 459–465.

55 R. Hao, R. J. Xing, Z. C. Xu, Y. L. Hou, S. Gao and S. H. Sun, *Adv. Mater.*, 2010, **22**, 2729–2742.

56 A. Rosencwaig and A. Gersho, *J. Appl. Phys.*, 1976, **47**, 64–69.

57 H. F. Zhang, K. Maslov, G. Stoica and L. V. Wang, *Nat. Biotechnol.*, 2006, **24**, 848–851.

58 G. Yao and L. V. Wang, *Appl. Opt.*, 2000, **39**, 659–664.

59 X. Wang, Y. Pang, G. Ku, X. Xie, G. Stoica and L. V. Wang, *Nat. Biotechnol.*, 2003, **21**, 803–806.

60 Y. Wang, X. Xie, X. Wang, G. Ku, K. L. Gill, D. P. O'Neal, G. Stoica and L. V. Wang, *Nano Lett.*, 2004, **4**, 1689–1692.

61 W. Lu, Q. Huang, G. Ku, X. Wen, M. Zhou, D. Guzatov, P. Brecht, R. Su, A. Oraevsky and L. V. Wang, *Biomaterials*, 2010, **31**, 2617–2626.

62 G. D. Moon, S. W. Choi, X. Cai, W. Li, E. C. Cho, U. Jeong, L. V. Wang and Y. Xia, *J. Am. Chem. Soc.*, 2011, **133**, 4762–4765.

63 Y. S. Chen, W. Frey, S. Kim, P. Kruizinga, K. Homan and S. Emelianov, *Nano Lett.*, 2011, **11**, 348–354.

64 J. Jackson and N. Halas, *J. Phys. Chem. B*, 2001, **105**, 2743–2746.

65 Z. Jiang and C. Liu, *J. Phys. Chem. B*, 2003, **107**, 12411–12415.

66 A. De La Zerda, C. Zavaleta, S. Keren, S. Vaithilingam, S. Bodapati, Z. Liu, J. Levi, B. R. Smith, T. J. Ma and O. Oralkan, *Nat. Nanotechnol.*, 2008, **3**, 557–562.

67 J. W. Kim, E. I. Galanzha, E. V. Shashkov, H. M. Moon and V. P. Zharov, *Nat. Nanotechnol.*, 2009, **4**, 688–694.

68 W. Dong, Y. Li, D. Niu, Z. Ma, J. Gu, Y. Chen, W. Zhao, X. Liu, C. Liu and J. Shi, *Adv. Mater.*, 2011, **23**, 5392–5397.

69 M. A. Nash, J. J. Lai, A. S. Hoffman, P. Yager and P. S. Stayton, *Nano Lett.*, 2010, **10**, 85–91.

70 Y. Jin, C. Jia, S. W. Huang, M. O'Donnell and X. Gao, *Nat. Commun.*, 2010, **1**, 41.

71 A. Gole, J. W. Stone, W. R. Gemmill, H. C. zur Loye and C. J. Murphy, *Langmuir*, 2008, **24**, 6232–6237.

72 H. M. Kim, H. Lee, K. S. Hong, M. Y. Cho, M. H. Sung, H. Poo and Y. T. Lim, *ACS Nano*, 2011, **5**, 8230–8240.

73 J. E. Lee, D. J. Lee, N. Lee, B. H. Kim, S. H. Choi and T. Hyeon, *J. Mater. Chem.*, 2011, **21**, 16869–16872.

74 C. Chandrana, P. Bevan, J. Hudson, I. Pang, P. Burns, D. Plewes and R. Chopra, *Phys. Med. Biol.*, 2011, **56**, 861–877.

75 S. Sundararajan, E. Tohno, H. Kamma, E. Ueno and M. Minami, *Radiat. Med.*, 2006, **24**, 108–114.

76 A. M. Tang, D. F. Kacher, E. Y. Lam, M. Brodsky, F. A. Jolesz and E. S. Yang, *Conf. Proc. IEEE Eng. Med. Biol. Soc.*, 2007, 2603–2606.

77 R. John, F. T. Nguyen, K. J. Kolbeck, E. J. Chaney, M. Marjanovic, K. S. Suslick and S. A. Boppart, *Mol. Imag. Biol.*, 2011, 1–8.

78 N. Rapoport, K. H. Nam, R. Gupta, Z. Gao, P. Mohan, A. Payne, N. Todd, X. Liu, T. Kim and J. Shea, *J. Controlled Release*, 2011, **153**, 4–15.

79 Z. Liu, T. Lammers, J. Ehling, S. Fokong, J. Bornemann, F. Kiessling and J. Gaetjens, *Biomaterials*, 2011, **32**, 6155–6163.

80 J. C. Park, M. K. Yu, G. I. An, S. I. Park, J. Oh, H. J. Kim, J. H. Kim, E. K. Wang, I. H. Hong and Y. S. Ha, *Small*, 2010, **6**, 2863–2868.

81 H. Xing, W. Bu, S. Zhang, X. Zheng, M. Li, F. Chen, Q. He, L. Zhou, W. Peng and Y. Hua, *Biomaterials*, 2012, **33**, 1079–1089.

82 K. Saatchi, P. Soema, N. Gelder, R. Misri, K. McPhee, J. H. E. Baker, S. Reinsberg, D. E. Brooks and U. O. Hafeli, *Bioconjugate Chem.*, 2012, **23**, 372–381.

83 X. Ma, Y. Zhao and X. J. Liang, *Acc. Chem. Res.*, 2011, **44**, 1114–1122.

84 S. Nie, Y. Xing, G. J. Kim and J. W. Simons, *Annu. Rev. Biomed. Eng.*, 2007, **9**, 257–288.

85 J. Xie, S. Lee and X. Chen, *Adv. Drug Delivery Rev.*, 2010, **62**, 1064–1079.

86 S. Mornet, S. Vasseur, F. Grasset and E. Duguet, *J. Mater. Chem.*, 2004, **14**, 2161–2175.

87 R. Cavaliere, E. C. Ciocatto, B. C. Giovanella, C. Heidelberger, R. O. Johnson, M. Margottini, B. Mondovi, G. Moricca and A. Rossi-Fanelli, *Cancer*, 1967, **20**, 1351–1381.

88 K. Overgaar and J. Overgaar, *Eur. J. Cancer*, 1972, **8**, 65–68.

89 A. K. Gupta and M. Gupta, *Biomaterials*, 2005, **26**, 3995–4021.

90 D. Yoo, J. H. Lee, T. H. Shin and J. Cheon, *Acc. Chem. Res.*, 2011, **44**, 863–874.

91 P. Drake, H. J. Cho, P. S. Shih, C. H. Kao, K. F. Lee, C. H. Kuo, X. Z. Lin and Y. J. Lin, *J. Mater. Chem.*, 2007, **17**, 4914–4918.

92 N. Prasad, K. Rathinasamy, D. Panda and D. Bahadur, *J. Mater. Chem.*, 2007, **17**, 5042–5051.

93 J. Jang, H. Nah, J. H. Lee, S. H. Moon, M. G. Kim and J. Cheon, *Angew. Chem.*, 2009, **121**, 1260–1264.

94 F. Sonvico, S. Mornet, S. Vasseur, C. Dubernet, D. Jaillard, J. Degrouard, J. Hoebeke, E. Duguet, P. Colombo and P. Couvreur, *Bioconjugate Chem.*, 2005, **16**, 1181–1188.

95 M. Creixell, A. C. Bohórquez, M. Torres-Lugo and C. Rinaldi, *ACS Nano*, 2011, **5**, 7124–7129.

96 J. R. McCarthy and R. Weissleder, *Adv. Drug Delivery Rev.*, 2008, **60**, 1241–1251.

97 S. Giri, B. G. Trewyn, M. P. Stellmaker and V. S. Y. Lin, *Angew. Chem., Int. Ed.*, 2005, **44**, 5038–5044.

98 A. Baeza, E. Guisasola, E. Ruiz-Hernández and M. Vallet-Regí, *Chem. Mater.*, 2012, **24**, 517–524.

99 G. von Maltzahn, J. H. Park, A. Agrawal, N. K. Bandaru, S. K. Das, M. J. Sailor and S. N. Bhatia, *Cancer Res.*, 2009, **69**, 3892.

100 H. Liu, D. Chen, L. Li, T. Liu, L. Tan, X. Wu and F. Tang, *Angew. Chem., Int. Ed.*, 2011, **50**, 891–895.

101 H. Ke, J. Wang, Z. Dai, Y. Jin, E. Qu, Z. Xing, C. Guo, X. Yue and J. Liu, *Angew. Chem.*, 2011, **123**, 3073–3077.

102 M. S. Yavuz, Y. Cheng, J. Chen, C. M. Cobley, Q. Zhang, M. Rycenga, J. Xie, C. Kim, K. H. Song and A. G. Schwartz, *Nat. Mater.*, 2009, **8**, 935–939.

103 J. H. Park, G. Von Maltzahn, M. J. Xu, V. Fogal, V. R. Kotamraju, E. Ruoslahti, S. N. Bhatia and M. J. Sailor, *Proc. Natl. Acad. Sci. U. S. A.*, 2009, **107**, 981–986.

104 G. Von Maltzahn, J. H. Park, K. Y. Lin, N. Singh, C. Schwöppe, R. Mesters, W. E. Berdel, E. Ruoslahti, M. J. Sailor and S. N. Bhatia, *Nat. Mater.*, 2011, **10**, 545–552.

105 S. P. Sherlock, S. M. Tabakman, L. Xie and H. Dai, *ACS Nano*, 2011, **5**, 1505–1512.

106 C. M. Hessel, V. P. Pattani, M. Rasch, M. G. Panthani, B. Koo, J. W. Tunnell and B. A. Korgel, *Nano Lett.*, 2011, **11**, 2560–2566.

107 J. D. Spikes and R. Livingston, *Adv. Radiat. Biol.*, 1969, **3**, 30–121.

108 T. Hasan, B. Ortel, A. C. E. Moor and B. W. Pogue, *Cancer Med.*, 2003, **7**, 537–548.

109 S. B. Brown, E. A. Brown and I. Walker, *Lancet Oncol.*, 2004, **5**, 497–508.

110 D. E. Dolmans, D. Fukumura and R. K. Jain, *Nat. Rev. Cancer*, 2003, **3**, 380–387.

111 U. Basu, I. Khan, A. Hussain, P. Kondaiah and A. R. Chakravarty, *Angew. Chem., Int. Ed.*, 2012, **51**, 2658–2661.

112 B. Jang, J. Y. Park, C. H. Tung, I. H. Kim and Y. Choi, *ACS Nano*, 2011, **5**, 1086–1094.

113 C. Wang, H. Tao, L. Cheng and Z. Liu, *Biomaterials*, 2011, **32**, 6145–6154.

114 M. Gary-Bobo, Y. Mir, C. Rouxel, D. Brevet, I. Basile, M. Maynadier, O. Vaillant, O. Mongin, M. Blanchard-Desce and A. Morère, *Angew. Chem.*, 2011, **123**, 11627–11631.

115 K. J. Son, H. J. Yoon, J. H. Kim, W. D. Jang, Y. Lee and W. G. Koh, *Angew. Chem., Int. Ed.*, 2011, **50**, 11968–11971.

116 A. C. S. Samia, X. Chen and C. Burda, *J. Am. Chem. Soc.*, 2003, **125**, 15736–15737.

117 M. F. Kircher, A. de la Zerda, J. V. Jokerst, C. L. Zavaleta, P. J. Kempen, E. Mittra, K. Pitter, R. Huang, C. Campos and F. Habte, *Nat. Med.*, 2012, **18**, 829–835.

118 E. S. Olson, T. Jiang, T. A. Aguilera, Q. T. Nguyen, L. G. Ellies, M. Scadeng and R. Y. Tsien, *Proc. Natl. Acad. Sci. U. S. A.*, 2010, **107**, 4311–4316.

119 S. Krasnici, A. Werner, M. E. Eichhorn, M. Schmitt-Sody, S. A. Pahernik, B. Sauer, B. Schulze, M. Teifel, U. Michaelis, K. Naujoks and M. Dellian, *Int. J. Cancer*, 2003, **105**, 561–567.

120 E. Connor, J. Mwamuka, A. Gole, C. J. Murphy and M. Whyatt, *Small*, 2005, **1**, 325–327.

121 K. Y. Huang, H. L. Ma, J. Liu, S. D. Huo, A. Kumar, T. Wei, X. Zhang, S. B. Jin, Y. L. Gan, P. C. Wang, S. T. He, X. N. Zhang and X. J. Liang, *ACS Nano*, 2012, **6**, 4483–4493.

122 B. D. Chithrani, A. A. Ghazani and W. C. W. Chan, *Nano Lett.*, 2006, **6**, 662–668.

123 A. Tkatchenko, H. Xie, Y. Liu, D. Coleman, J. Ryan, W. Glomm, M. Shipton, S. Franzen and D. Feldheim, *Bioconjugate Chem.*, 2004, **15**, 482–490.

124 J. Rejman, W. Oberle, I. S. Zuhorn and D. Hoekstra, *Biochem. J.*, 2004, **377**, 159–169.

125 W. H. de Jong, W. I. Hagens, P. Krystek, M. C. Burger, A. J. A. M. Sips and R. E. Geertsma, *Biomaterials*, 2008, **29**, 1912–1919.

126 E. A. Gratton, P. Polhaus, J. Lee, J. Guo, M. Cho and J. DeSimone, *J. Controlled Release*, 2007, **121**, 10–18.